Available online at www.sciencedirect.com
SCIENCE DIRECT
Journal of Power Sources 158 (2006) 654–658
JOURNAL OF POWER SOURCES
www.elsevier.com/locate/jpowsour

Short communication

Synthesis and characterization of high tap-density layered $Li[Ni_{1/3}Co_{1/3}Mn_{1/3}]O_2$ cathode material via hydroxide co-precipitation

Xufang Luo [a], Xianyou Wang [a,*], Li Liao [a], Sergio Gamboa [b], P.J. Sebastian [b]

[a] *College of Chemistry, Xiangtan University, Hunan 411105, China*
[b] *Solar-Hydrogen-Fuel Cell Group, CIE-UNAM, Temixco 62580, Morelos, Mexico*

Received 2 September 2005; accepted 28 September 2005
Available online 28 November 2005

Abstract

$Li[Ni_{1/3}Co_{1/3}Mn_{1/3}]O_2$ was prepared by mixing uniform co-precipitated spherical metal hydroxide $(Ni_{1/3}Co_{1/3}Mn_{1/3})(OH)_2$ with 7% excess LiOH followed by heat-treatment. The tap-density of the powder obtained was 2.38 g cm^{-3}, and it was characterized using X-ray diffraction (XRD), particle size distribution measurement, scanning electron microscope-energy dispersive spectrometry (SEM-EDS) and galvanostatic charge–discharge tests. The XRD studies showed that the material had a well-ordered layered structure with small amount of cation mixing. It can be seen from the EDS results that the transition metals (Ni, Co and Mn) in $Li[Ni_{1/3}Co_{1/3}Mn_{1/3}]O_2$ are uniformly distributed. Initial charge and discharge capacity of 185.08 and 166.99 mAh g^{-1} was obtained between 3 and 4.3 V at a current density of 16 mA g^{-1}, and the capacity of 154.14 mAh g^{-1} was retained at the end of 30 charge–discharge cycles with the capacity retention of 93%.

Keywords: Lithium ion battery; $Li[Ni_{1/3}Co_{1/3}Mn_{1/3}]O_2$; Co-precipitated spherical metal hydroxide; Capacity retention; Discharge capacity

1. Introduction

Lithium-ion batteries (LIB) with high energy density, power capability and long cycle life are used to power portable electronic devices such as cellular phones and laptop computers and have long been considered as possible power source for electric vehicle (EV), hybrid electric vehicle (HEV) and high efficiency energy-storage systems [1]. The first commercial LIB introduced in 1990 by SONY, used $LiCoO_2$ as a cathode, and this material continues to be used in more than 90% of LIB manufactured despite the high cost and safety hazards associated with cobalt [2,3]. Considerable effort has been expended over the past decade to find possible alternatives to $LiCoO_2$ in LIB. Recently, the $Li[Ni_xCo_{1-2x}Mn_x]O_2$ system used in LIB was reported to be one of attractive cathode materials [4–8]. Among them, $Li[Ni_{1/3}Co_{1/3}Mn_{1/3}]O_2$, a special case in which x is 1/3, was first synthesized by Ohzuku and Makimura [9] in 2001, has attracted significant interest in the investigation of cathode materials of LIB due to its stable cycling performances, good thermal stability and excellent rate capability. It is considered to be one of the best candidates for the positive electrode material for hybrid electric vehicle power source systems by Amine and co-workers [10] and it was reported that the rechargeable capacity of $Li[Ni_{1/3}Co_{1/3}Mn_{1/3}]O_2$ was 160 mAh g^{-1} when the cell operated at 2.5–4.4 V and more than 200 mAh g^{-1} on the voltage range of 2.8–4.6 V [11,12]. It is well known that the physical properties of one material, such as morphology, particle size distribution, tap-density and specific surface area is very important if it is used in practical LIB. Therefore, the uniform distribution of spherical powders with high tap-density is the key for $Li[Ni_{1/3}Co_{1/3}Mn_{1/3}]O_2$ in massive application. In this paper, a metal hydroxide obtained via co-precipitation method was employed to prepare high tap-density $Li[Ni_{1/3}Co_{1/3}Mn_{1/3}]O_2$ powders, and its structural, morphological and electrochemical behaviors were studied.

2. Experimental

The precursor $(Ni_{1/3}Co_{1/3}Mn_{1/3})(OH)_2$ was prepared in following manner. The stoichiometric amounts of $NiSO_4{\cdot}6H_2O$, $CoSO_4{\cdot}7H_2O$ and $MnSO_4{\cdot}H_2O$ were dissolved together in distilled water (cationic ratio of Ni:Co:Mn = 1:1:1) and the concentration of the total metal sulfate was 2 mol L^{-1}. The aqueous

* Corresponding author. Tel.: +86 732 8293371; fax: +86 732 8292061.
E-mail address: wxianyou@yahoo.com (X. Wang).

0378-7753/$ – see front matter © 2005 Elsevier B.V. All rights reserved.
doi:10.1016/j.jpowsour.2005.09.047

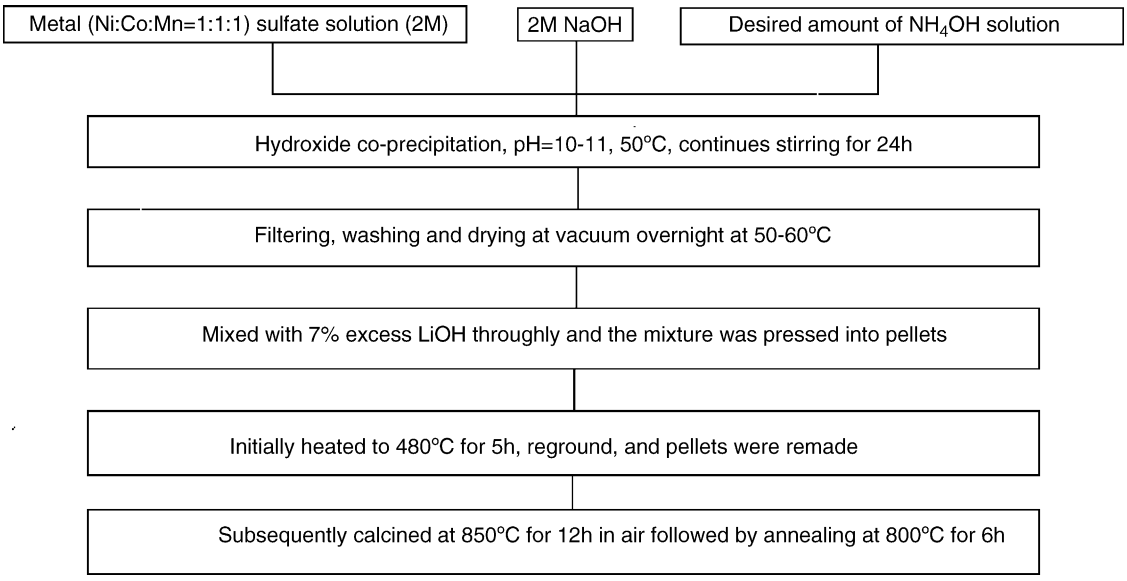

Fig. 1. Synthetic route of $Li[Ni_{1/3}Co_{1/3}Mn_{1/3}]O_2$ powder.

solution was precipitated by adding NaOH solution (aq.) of 2 mol L^{-1} and the desired amount of NH_4OH solution (aq.) separately under an argon atmosphere along with continued stirring. The solution was maintained at 50 °C for 24 h and the pH was controlled to 10–11. After filtering, washing and drying in a vacuum at 50–60 °C overnight, the obtained precursor powder was mixed with 7% excess LiOH (excess amount of Li salts was used to compensate possible Li loss during the calcination) using a ball mill and the powder was pressed into pellets. The pellets were initially heated to 480 °C for 5 h, and then reground. Pellets were remade and subsequently calcined at 850 °C for 12 h in air followed by annealing at 800 °C for 6 h. All the steps are summarized in Fig. 1.

The as-prepared powders were observed using a scanning electron microscope (SEM, JSM-6380LV, JEOL) equipped with energy dispersive spectrometry (EDS, Oxford). Powder X-ray diffraction was carried out using a Cu Kα radiation of Rigaku D/max 2550 diffractometer. Silicon powder was used as an internal standard for the calculation of lattice parameters. The particle size distribution was measured by Mastersizer 2000 (MS2000, Malvern).

The cathode was prepared by mixing the active material with carbon black and PTFE in a weight ratio of 75:15:10. The mixture was pressed onto stainless steel mesh used as the current collector and dried under vacuum at 120 °C for 24 h. The laboratory pouch cells consisting of the cathode, the lithium foil as an anode and 1 M $LiPF_6$-EC/DMC (1:1, v/v) as the electrolyte were assembled in an argon-filled glove box. Cycle tests were performed on the cells between 3 and 4.3 V at 0.1*C* of a constant current at 30 °C with a BTS-51800 Neware Battery Testing System (160 mA g^{-1} was assumed to be 1*C* rate).

3. Results and discussion

Fig. 2 shows the XRD pattern of $Li[Ni_{1/3}Co_{1/3}Mn_{1/3}]O_2$. This figure reveals that the as-synthesized powder has the typical structure of a hexagonal α-$NaFeO_2$ type with a space group of $R\bar{3}m$ (No. 166). The diffraction peaks are quite narrow, indicating high crystallinity and no impurity diffraction peak was observed. As seen from Fig. 2, the splits in the (0 0 6)/(1 0 2) and (1 0 8)/(1 1 0) doublets indicate the formation of a highly ordered layer structure [13]. A partial interchange of occupancy of Li and transition-metal ions especially for the divalent nickel (Ni^{2+}) because the radius of the Ni^{2+}($r_{Ni^{2+}} = 0.69$ Å) is close to that of the Li^+ ($r_{Li^+} = 0.76$ Å), would give rise to cation mixing in the structure, can deteriorate battery performances [13,14]. Some researchers [15,16] used the high-integrated intensity ratio of the I_{003}/I_{004} to indicate the cation mixing of the layered structure. Generally, when $I_{003}/I_{004} > 1.2$, the cation mixing is small with good layered structure. Based on Fig. 2, the hexagonal lattice parameters were determined to be $a = 2.8602$ Å, $c = 14.2260$ Å and $c/a = 4.9738$, calculated by using silicon powder as an

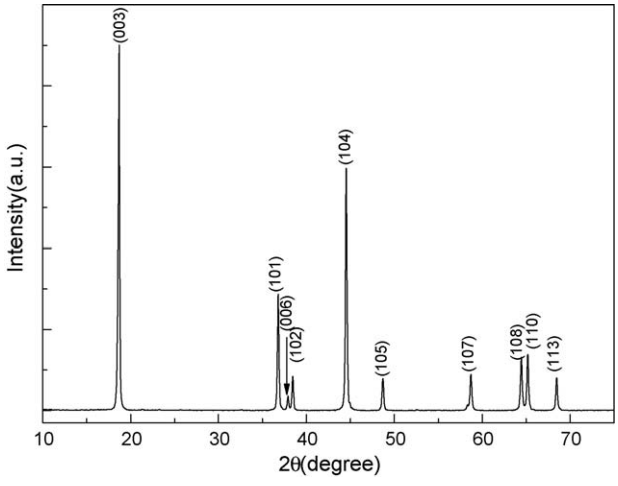

Fig. 2. X-ray diffraction pattern of $Li[Ni_{1/3}Co_{1/3}Mn_{1/3}]O_2$ powder prepared by calcinations of $(Ni_{1/3}Co_{1/3}Mn_{1/3})(OH)_2$ and appropriate amounts of LiOH at 850 °C for 12 h and then annealed at 800 °C for 6 h.

Table 1
Calculated structure parameters and tap-density for the synthesized $Li[Ni_{1/3}Co_{1/3}Mn_{1/3}]O_2$

Sample	$Li[Ni_{1/3}Co_{1/3}Mn_{1/3}]O_2$
a(Å)	2.8602
c(Å)	14.2260
c/a	4.9738
Volume (Å^3)	100.7891
$I_{(003)}/I_{(104)}$	1.5624
R	0.4073
Tap-density (g cm^{-3})	2.38

internal standard and are tabulated in Table 1. These data match well with the values observed by Kim and Chung ($a = 2.8622$ Å, $c = 14.2502$ Å) [17] and Park et al. ($a = 2.8604$ Å, $c = 14.2405$ Å) [18]. The I_{003}/I_{004} value of 1.56, indicating no undesirable cation mixing, is observed in this sample. In addition, According to Dahn et al. [19,20], the R factor ($R = (I_{012} + I_{006})/I_{101}$) is an indicator of hexagonal ordering, the lower the R-value, the better the hexagonal ordering. This sample has a low R-value of 0.40, indicating good hexagonal ordering of its lattice. All the results mentioned above clearly confirmed the well-ordered layered structure of the synthesized powder.

Scanning electron microscopy (SEM) images of the $(Ni_{1/3}Co_{1/3}Mn_{1/3})(OH)_2$ powder at different magnifications are illustrated in Fig. 3 and its particle size distribution is shown in Fig. 4. As is well known, particle shape and size of cathode material can affect the energy density in practical use, so controlling particle morphology is very important. Dahn and co-workers [21] reported that larger particles have a higher tap-density. As can be seen in Figs. 3 and 4, a large number of needle-shaped nano-rods form on circular and uniform primary particles with an average size of about 1–2 μm, the majority of which are aggregated to form spherical secondary particles. The average size of the secondary particles is about 15 μm. This larger size of the precursor may be due to the lower pH during

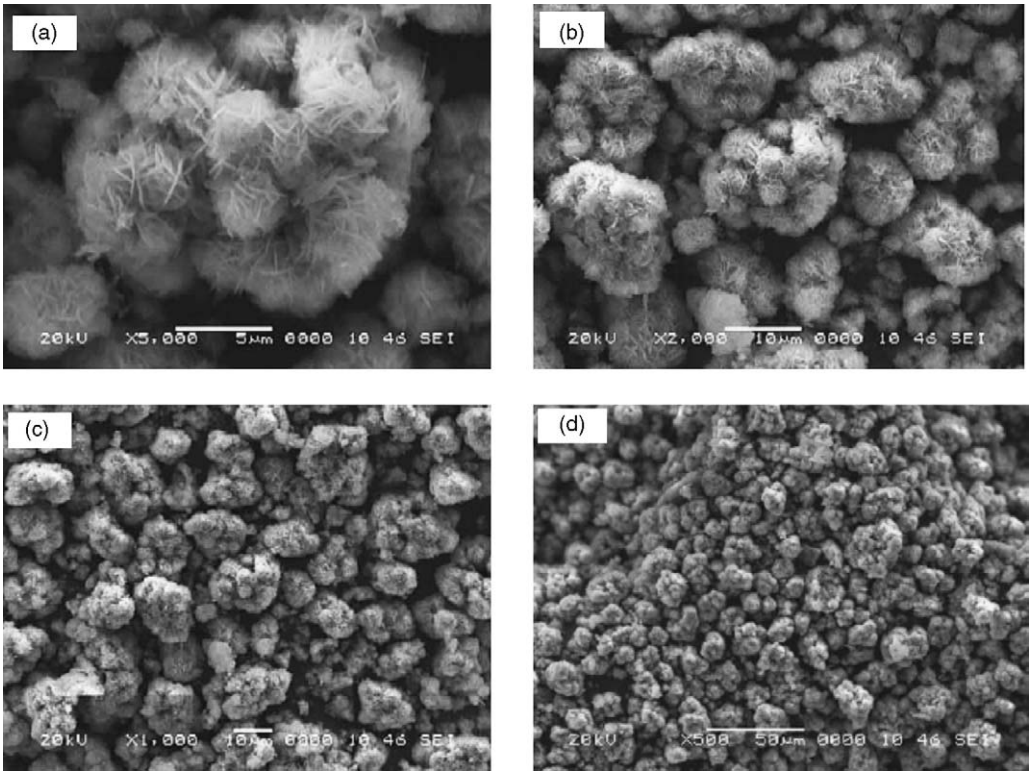

Fig. 3. SEM images of $(Ni_{1/3}Co_{1/3}Mn_{1/3})(OH)_2$ precursor at different magnifications. (a) ×5000; (b) ×2000; (c) ×1000 and (d) ×500.

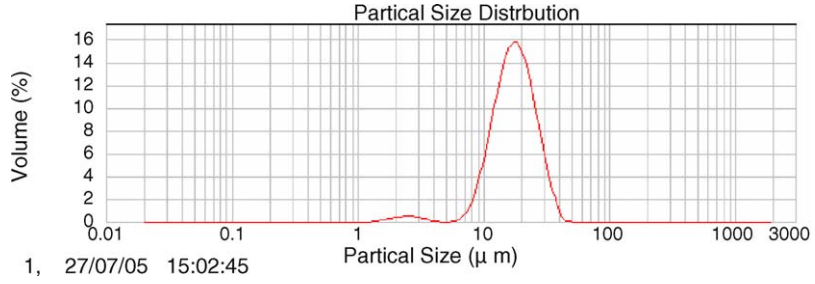

Fig. 4. The particle size distribution of $(Ni_{1/3}Co_{1/3}Mn_{1/3})(OH)_2$ precursor prepared by hydroxide co-precipitation.

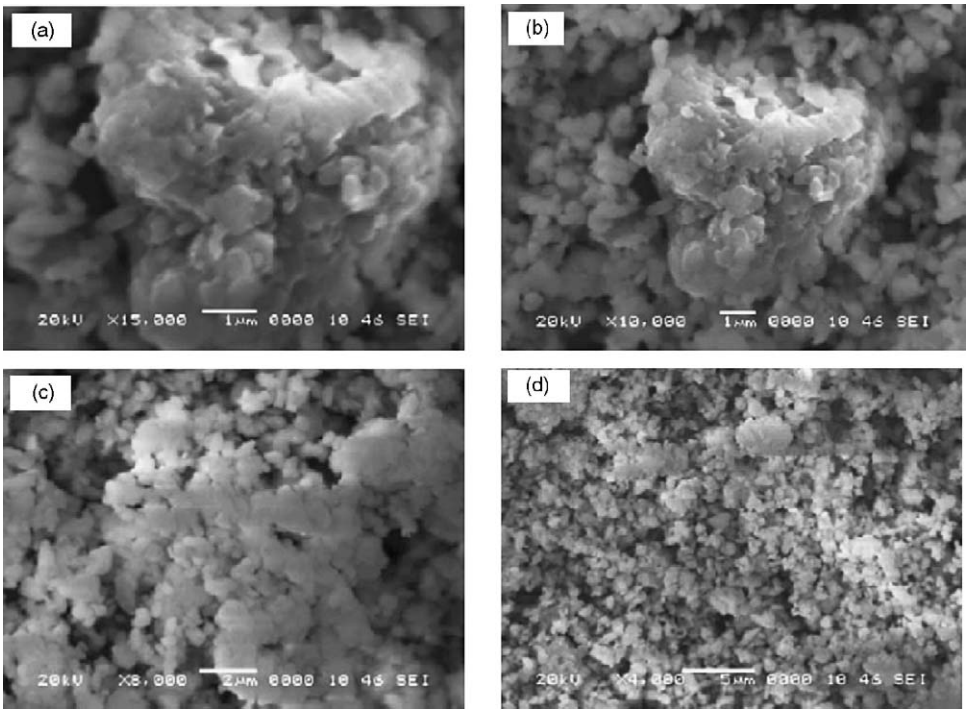

Fig. 5. SEM images of $Li[Ni_{1/3}Co_{1/3}Mn_{1/3}]O_2$ powder at different magnifications. (a) ×15,000; (b) ×10,000; (c) ×8000 and (d) ×4000.

the precipitation than other paper [22]. Fig. 5 shows the SEM images of $Li[Ni_{1/3}Co_{1/3}Mn_{1/3}]O_2$ at different magnifications. Though the spherical shape is not apparent compared to the precursor particles, the tap-density is up to 2.38 g cm^{-3}, which is close to that of commercialized $LiCoO_2$. We consider that the uniform spherical precursor can result in high tap-density of the final product $Li[Ni_{1/3}Co_{1/3}Mn_{1/3}]O_2$. The EDS results show homogeneous element distribution in the precipitation.

Fig. 6a shows the cell voltage plotted versus specific gravimetric capacity for the first and the 30th charge–discharge cycle operated at a constant current density of 16 mA g^{-1} between 3 and 4.3 V versus Li at 30 °C and Fig. 6b shows cycling performance of the material up to 30 cycles. The $Li[Ni_{1/3}Co_{1/3}Mn_{1/3}]O_2$ electrode delivers an initial discharge capacity of 166.99 mAh g^{-1} with an irreversible capacity loss of 24 mAh g^{-1} during the first charge and discharge cycle and the first coulombic efficiency is 90.23%. The irreversible capacity loss of 24 mAh g^{-1} was probably due to the formation of a solid electrolyte interface (SEI) on the surface of cathode active materials. The charge and discharge capacities on the 30th cycle are 159.09 and 154.14 mAh g^{-1}, respectively, with a coulombic efficiency of 96.87%. The capacity retention at the 30th cycle was 93%. The coulombic efficiencies of all the cycles are above 96% except the first cycle. The excellent cycling stability of the active material may be due to the needle-shaped nanorods of the spherical primary particles of the precursor and the highly ordered layered structure as well as the high tap-density of the final $Li[Ni_{1/3}Co_{1/3}Mn_{1/3}]O_2$ powder with small amounts of cation mixing. However, the rate capability of the active material not shown here is not as good as expected. We suggest that innovative synthesis and improved heat-treatment or ion substitution is an effective way to improve the rate capability and we will

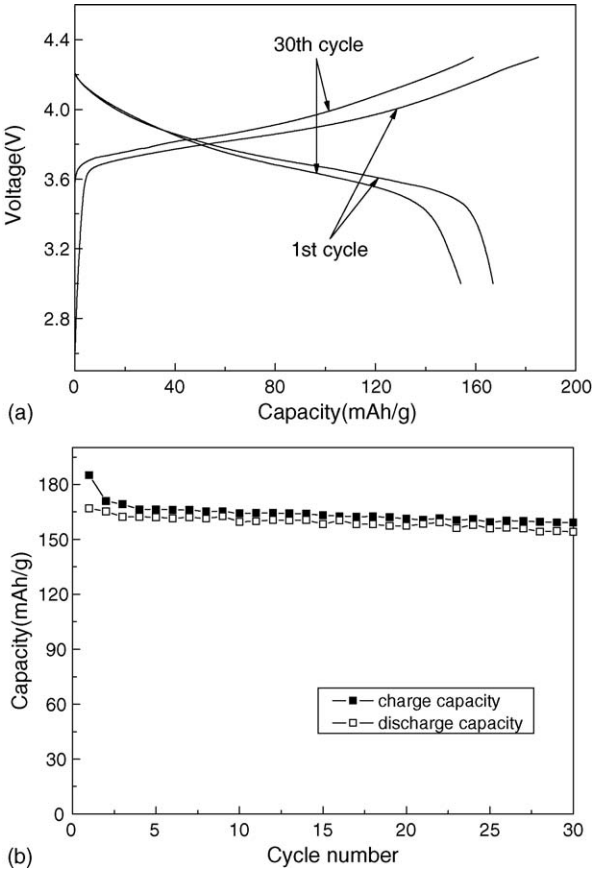

Fig. 6. The first and the 30th charge–discharge profiles (a) and its cycling performance (b) of a $Li/Li[Ni_{1/3}Co_{1/3}Mn_{1/3}]O_2$ cell (3–4.3 V) operated at 16 mA g^{-1} at 30 °C.

discuss this in a later paper. On the other hand, as mentioned above, tap-density of the active material is very important for the capacity of battery. Especially for practical applications, the capacity, cyclability, rate capability as well as the tap-density of $Li[Ni_{1/3}Co_{1/3}Mn_{1/3}]O_2$ should be considered comprehensively. In this paper, the as-prepared active material has a high discharge capacity, excellent cyclability and capacity retention high tap-density, thus it will be the most promising alternative to $LiCoO_2$ for advanced LIB.

4. Conclusions

$Li[Ni_{1/3}Co_{1/3}Mn_{1/3}]O_2$ prepared by hydroxide co-precipitation shows a well-ordered layered structure and a high tap-density ($2.38\,g\,cm^{-3}$), which is close to that of commercialized $LiCoO_2$. The $Li[Ni_{1/3}Co_{1/3}Mn_{1/3}]O_2$ electrode exhibits a high charge and discharge capacity of 185.08 and 166.99 mAh g^{-1}, respectively, between 3 and 4.3 V at a current density of 16 mA g^{-1} at 30 °C and retains 154.14 mAh g^{-1} at the end of 30 cycles. The coulombic efficiencies of all the cycles are above 96% except the first cycle and the discharge capacity loss after 30 cycles is only 7% of the first cycle. It is concluded that hydroxide co-precipitation is an excellent method to synthesize uniform spherical precursor $(Ni_{1/3}Co_{1/3}Mn_{1/3})(OH)_2$ powder, which ultimately results in good performance of the final product $Li[Ni_{1/3}Co_{1/3}Mn_{1/3}]O_2$.

Acknowledgements

This work was financially supported by the Key Project of Department of Science and Technology of Hunan Province under the grant no. 05GK2015, the Key Project of Department of Education of Hunan Province under the grant no. 04A054, and the Key Project of Ministry of Education of China under the grant no. 205109.

References

[1] I.B. Weinstock, J. Power Sources 110 (11) (2002) 471–474.
[2] R.J. Brodd, K.R. Bullock, R.A. Leising, R.L. Middaugh, J.R. Miller, E. Takeuchic, J. Electrochem. Soc. 151 (3) (2004) K1–K11.
[3] B. Ammundsen, J. Paulsen, Adv. Mater. 13 (12–13) (2001) 943–956.
[4] Z. Lu, D.D. MacNeil, J.R. Dahn, Elecrtrochem. Solid State Lett. 4 (12) (2001) A200–A203.
[5] D.D. MacNeil, Z. Lu, J.R. Dahn, J. Electrochem. Soc. 149 (10) (2002) A1332–A1336.
[6] S. Jouanneau, D.D. MacNeil, Z. Lu, S.D. Beattie, G. Murphy, J.R. Dahn, J. Electrochem. Soc. 150 (10) (2003) A1294–A1298.
[7] S. Jouanneau, K.W. Eberman, L.J. Krause, J.R. Dahn, J. Electrochem. Soc. 150 (12) (2003) A1637–A1642.
[8] S. Jouanneau, W. Bahmet, K.W. Eberman, L.J. Krause, J.R. Dahn, J. Electrochem. Soc. 151 (11) (2004) A1789–A1796.
[9] T. Ohzuku, Y. Makimura, Chem. Lett. 7 (2001) 642–643.
[10] G. Henriksen, K. Amine, J. Liu, P. Nelson, Abstract 255, 204th Meeting of The Electrochemical Society, Orlando, 12–16 October, 2003.
[11] N. Yabuuchi, T. Ohzuku, J. Power Sources 119–121 (2003) 171–174.
[12] K.M. Shaju, G.V. Subba Rao, B.V.R. Chowdari, Electrochim. Acta 48 (2002) 145–151.
[13] A. Rougier, P. Gravereau, C. Delmas, J. Electrochem. Soc. 143 (4) (1996) 1168–1175.
[14] J. Baker, R. koksbang, M.Y. Saidi, Solid State Ionics 89 (1–2) (2005) 25–35.
[15] Y.Gao, M. Yakovleva, H.H. Wang, J.F. Engel, U.S. Patent, 6,620,400 (2003).
[16] Z.L. Liu, A.S. Yu, J.Y. Lee, J. Power Sources 81–82 (1999) 416–419.
[17] J.M. Kim, H.T. Chung, Electrochim. Acta 49 (2004) 937–944.
[18] S.H. Park, H.S. Shin, S.T. Myung, C.S. Yoon, K. Amine, Y.K. Sun, Chem. Mater. 17 (2005) 6–8.
[19] J.R. Dahn, U. von Sacken, C.A. Michal, Solid State Ionics 44 (1–2) (1990) 87–97.
[20] J.N. Reimers, E. Rossen, C.D. Jones, J.R. Dahn, Solid State Ionics 61 (4) (1993) 335–344.
[21] J. Jouanneau, K.W. Ekerman, L.J. Krause, J.R. Dahn, J. Electrochem. Soc. 150 (12) (2003) A1637–A1642.
[22] M.H. Lee, Y.J. Kang, S.T. Myung, Y.K. Sun, Electrochim. Acta 50 (2004) 939–948.